ELSEVIER

Ultrasonic Measurements on Hydrating Cement Slurries

Onset of Shear Wave Propagation

Ralph D'Angelo, Thomas J. Plona, Lawrence M. Schwartz, and Peter Coveney
Schlumberger-Doll Research, Ridgefield, Connecticut; and Schlumberger Cambridge Research, Cambridge, England

The ultrasonic properties of three oil field cement slurries are studied during the early stages of the hydration process. As a percolating solid framework is established, the slurries develop mechanical integrity and shear waves begin to propagate. This transition is also apparent in the behavior of the compressional wave, but is considerably more clear-cut in the shear signals. For the three samples examined here, the ratios of the shear wave onset times are in good agreement with the corresponding ratios of the American Petroleum Institute (API) thickening times. ADVANCED CEMENT BASED MATERIALS 1995, 2, 8–14

KEY WORDS: Hydrating slurries, Shear waves, Ultrasonics

Among the most important properties of oil well cements is the early time solidification rate after the initial slurry is prepared [1]. On the one hand, the mixture must remain in its fluid phase long enough to ensure that the slurry can be pumped easily into the bore hole annulus; on the other hand, once the cement has been pumped, it should set as rapidly as possible to prevent blowouts and avoid delay at the well site. Once set in the well bore, the cement forms a hydraulic seal against the migration of formation fluids. In addition, the cement provides mechanical support for the casing string and protects it against corrosion by the formation fluids.

An empirical measure of the time required for cement slurries to set is given by the American Petroleum Institute (API) thickening time [2]. Here, a device known as a consistometer is used to measure the torque required to stir the slurry at a constant rate. The cure time at which this torque reaches a prescribed value is then taken as the thickening time. Unfortunately, this measurement is not directly connected with any simple physical characteristic of the hydrating material. By contrast, acoustic experiments are readily interpreted in terms of the bulk and shear moduli of the composite. Indeed, ultrasonic measurements have often been used to estimate the mechanical properties of the hardened composite, and also to monitor the properties of the hydrating paste [3–8]. Most of this work has involved the measurement of compressional wave speeds. There is, however, a study by Stepišnik et al. [9] in which reflection techniques are used to study the onset of shear wave propagation. Also relevant to our research is the work of Hannant and coworkers [10–12], in which extremely low amplitude (≤ 0.05 μm) and essentially static displacements were used to measure the slurry's shear modulus at very early stages of the curing process. More recently, Sayers and Grenfell [13] have used the experimental techniques developed in this article to examine the behavior of the Poisson ratio, ν, during cement hydration. They find that ν decreases from $\nu = 0.50$, characteristic of a fluid, to values below 0.35, which are reasonable for porous solids.

On physical grounds, acoustic measurements are appealing because one expects to see rapid changes as the slurry evolves from its initial state, in which the solid clinker particles are suspended in a complex water-gel fluid, to its final solid configuration. It is only when the growing solid network first percolates (i.e., spans the system) that shear waves are expected to propagate. From this viewpoint, it may prove fruitful to analyze the shear wave transition in terms of recently developed dynamical models of the hydration process [14,15]. Indeed, Bentz et al. [16] find a striking similarity between the behavior of the percolation threshold in a three-dimensional cellular automaton simulation and the onset of shear wave energy in a hydrating cement slurry. In contrast to the shear wave, compressional waves can, in principle, propagate through the initial suspension. (In practice, however, we will see that it is sometimes difficult to detect compressional signals at early cure times.) At the onset of solidification, we expect a marked, but continuous in-

Address correspondence to: Lawrence M. Schwartz, Schlumberger-Doll Research, Old Quarry Road, Ridgefield, Connecticut 06877-4108.
Received October 15, 1993; Accepted January 3, 1994

ISSN 1065-7355/95/$9.50
SSDI 1065-7355(94)00015-6

crease in the compressional wave speed, as both the bulk and shear moduli increase in value.

In this study we examine in detail the behavior of shear and compressional propagation during the first 24 hours of hydration for three oil field cement slurries. Indeed, we propose a new, physically motivated definition of the cement set point, or thickening time, as the time it takes for the slurry to reach the percolation threshold. (This does not imply that it should be the same numerical value as in other definitions.) We believe that remote ultrasonic sensing of the shear wave onset will be valuable in oil field applications where, as indicated above, the monitoring of cement hydration times is of great importance.

Experimental Procedure

We designed an acquisition system (Figure 1) that allowed us to make direct and accurate ultrasonic measurements on hydrating cement paste. In addition, we monitored the temperature of the slurry as an indicator of the level of chemical activity. The three cement slurries chosen for this study cover a fairly wide range of thickening times. After being mixed according to API SPEC-10 instructions for class H cement, each slurry was poured into a lucite cell whose walls were 2.54 cm thick to buffer internal acoustic reflections. The volume occupied by the slurry was 15.24 × 12.70 × 1.27 cm. Attached to the outer walls of the cell were 2.54-cm

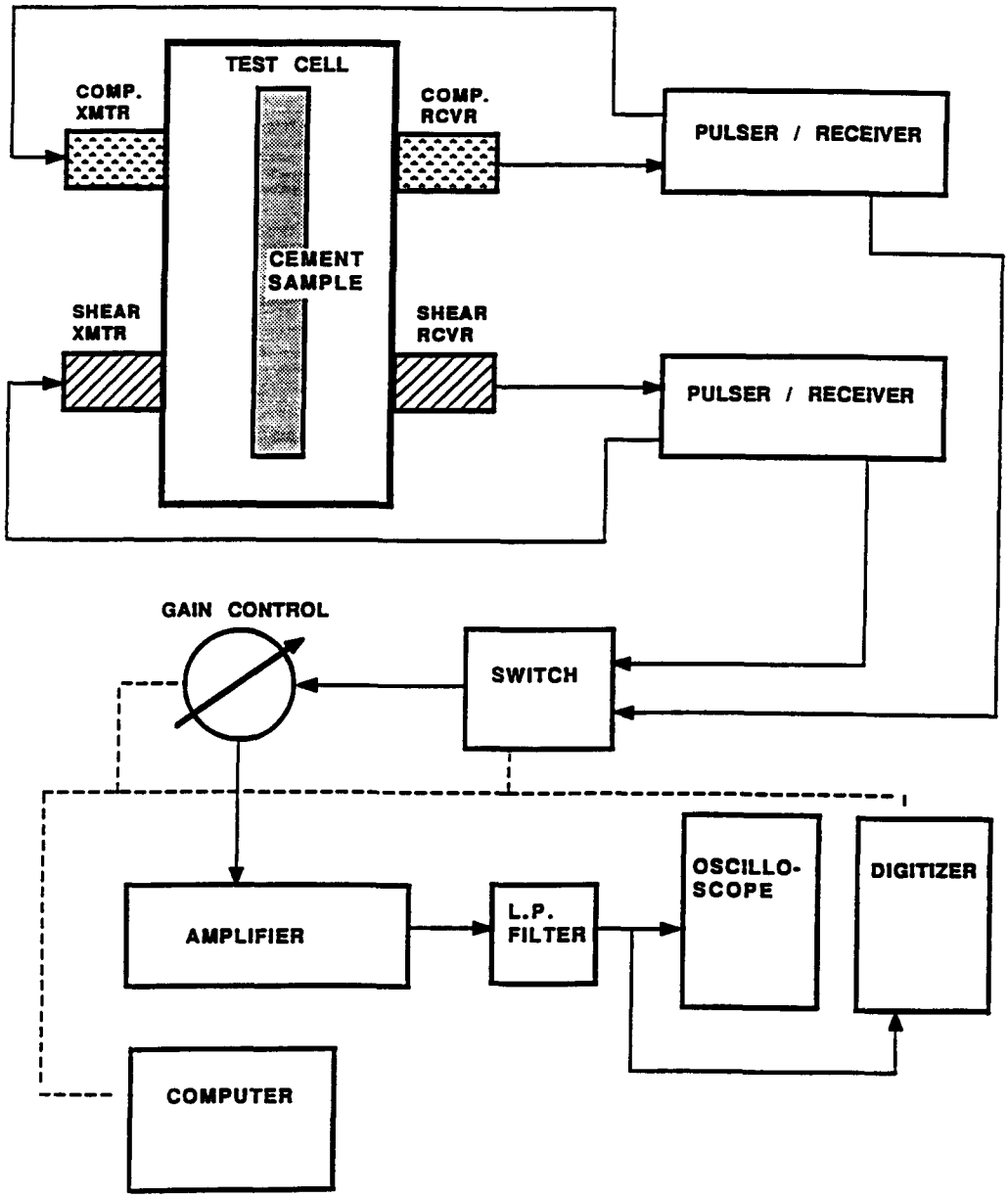

FIGURE 1. Schematic representation of the computer controlled data acquisition system for through-transmission of shear and compressional ultrasonic signals.

Advn Cem Bas Mat
1995;2:8–14

diameter, 1 MHz (center frequency) broad-band compressional (P) and shear (S) transducers. The transducers are similar to those used in standard ultrasonic nondestructive evaluation. The P and S transducers were fired simultaneously every 5 ms by two Panametrics pulser-receiver boxes. Once every 5 minutes the P and S signals were fed sequentially into an automatic gain control system, displayed on an oscilloscope screen, digitized, and stored. The acquisition system was controlled by a micro-VAX II over an IEEE-488 general purpose interface bus. The slurry temperature was measured continuously and stored at the same 5-minute intervals.

Experimental Results

The temperature variation, as a function of cure time, is shown for the three cements in Figure 2. These curves are similar to corresponding data available in the cement hydration literature [3–6]. All three samples show a pronounced rise in temperature after mixing, followed by a decrease. Note that within the first 24 hours the temperature curves all remain well above room temperature (roughly 21°C). The temperature rise is most dramatic for the Snocrete slurry and is slowest for the neat Cemoil (Cemoil[1]), although the latter sample does show the highest peak.

The general features of the ultrasonic waveforms collected in the first 24 hours are displayed (at 1-hour intervals) in Figures 3 and 4. The shear and compressional data (as collected) are shown, respectively, in 40 and 20 μs windows whose position is chosen to show the arrival of principal interest. It is clear from Figure 3 that shear waves do not propagate in the earliest stages of the curing process. In each case we see a clear shear wave onset, after which the waveforms move rapidly toward shorter arrival times as the cure matures. Turning to Figure 4, we see that, as expected, the shear wave onset is associated with a decrease in the compressional wave arrival times. While both the P and S waveforms show the signatures of a transition to a percolating solid frame, the effect is much clearer in the shear wave data. Indeed, in the case of Cemoil + $CaCl_2$ (Cemoil[2]), the P wave itself is barely evident for the first 4 hours of the cure. Clearly, in this case, to obtain an accurate estimate of changes in the P velocity would be quite difficult. In connection with this behavior, it should be mentioned that the API mixing procedure does not call for the de-airing of the slurry. Air bubbles may be causing large attenuation at the early stages of the Cemoil[2] cure; such behavior has been noted in Keating et al. [12].[1]

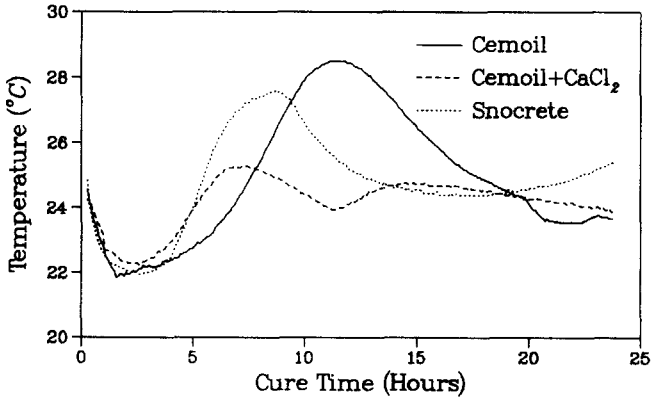

FIGURE 2. Temperature (°C) as a function of cure time for the three cement samples.

To derive a shear onset time from the ultrasonic waveforms, we have developed an automated processing algorithm that scans each waveform and locates the time of the first peak that exceeds a preset threshold. If a cycle skip occurred, the data were time shifted to make the complete velocity curve continuous. To facilitate the detection of weak signals (near the onset), we employed a 50 → 300 kHz bandpass filter to eliminate spurious components from the waveforms. The automatic detection of shear arrivals is then quite straightforward. The onset times derived from the filtered waveforms are given in Table 1. In Figure 5 we show the P and S velocities (obtained from the filtered waveforms) as a function of cure time for the three cements. The onset times listed in Table 1 correspond to the times at which the amplitudes of the three shear velocity curves drop to zero. Turning to the compressional velocities, we see that Cemoil[1] and Snocrete curves exhibit the kind of smooth transition to be expected based on the data presented in Figure 4. By contrast, the early time behavior of the Cemoil[2] curve is rather different because of the very weak compressional signals noted in Figure 4.

To examine the shear wave onset in more detail, we looked at the energy transmitted in the P and S waves. Here we begin with the power spectrum (i.e., the square magnitude of the waveform Fourier transform). For example, in Figure 6 we show the power spectra associated with shear arrivals for Cemoil[1] cement after cure times of 8, 12, 16, and 20 hours. In the early stages of the cure, the wave trains are quite broad and their frequency content is correspondingly narrow. As the cure proceeds, the shear arrivals tighten considerably and their power spectra broaden. Qualitatively similar behavior is seen in the shear spectra of the other cements. In Figure 7 we follow the evolution of the transmitted energy at 450 and 300 kHz, frequencies

[1] See Figure 2a of ref 12. Here, as in Cemoil[2], the cement is a class G accelerated with $CaCl_2$.

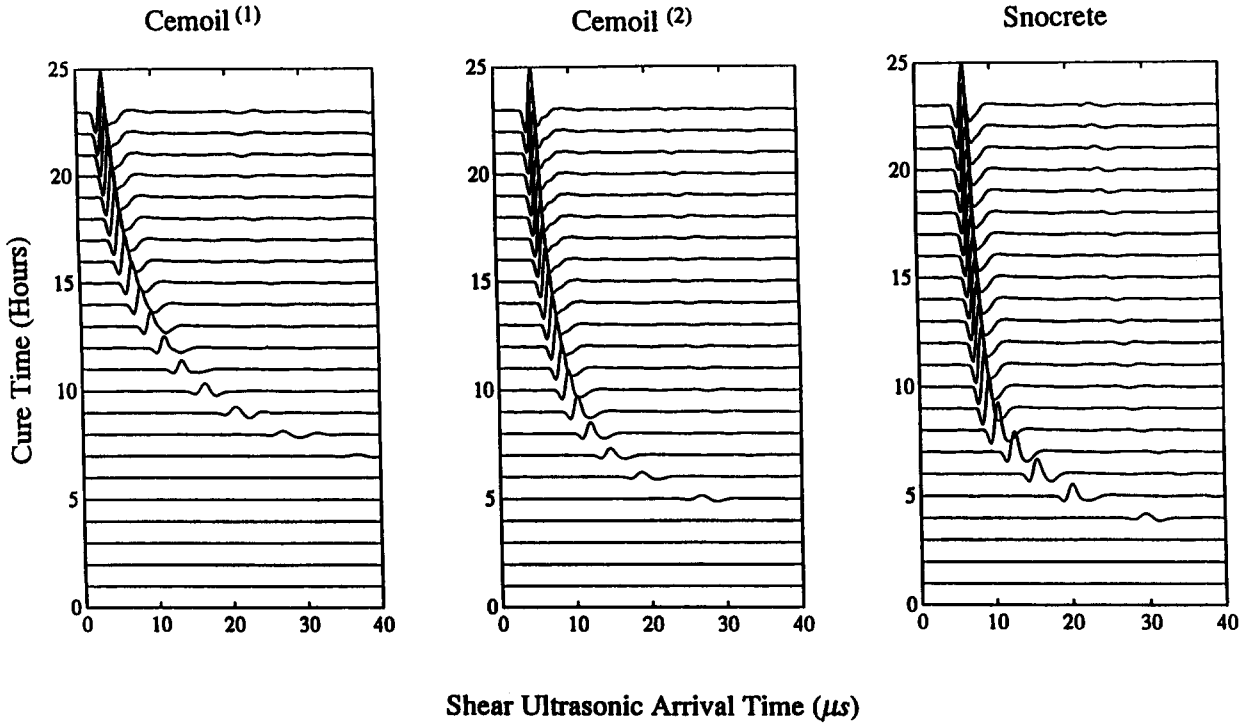

FIGURE 3. The raw shear wave arrivals are shown for the three cement samples. The number on the vertical axis is the number of cure hours. Only 40 milliseconds are shown in each case; the initial positions of the windows (i.e., the times at which we begin to display the data) are 43 (Cemoil$^{(1)}$), 43 (Cemoil$^{(2)}$), and 58 milliseconds (Snocrete).

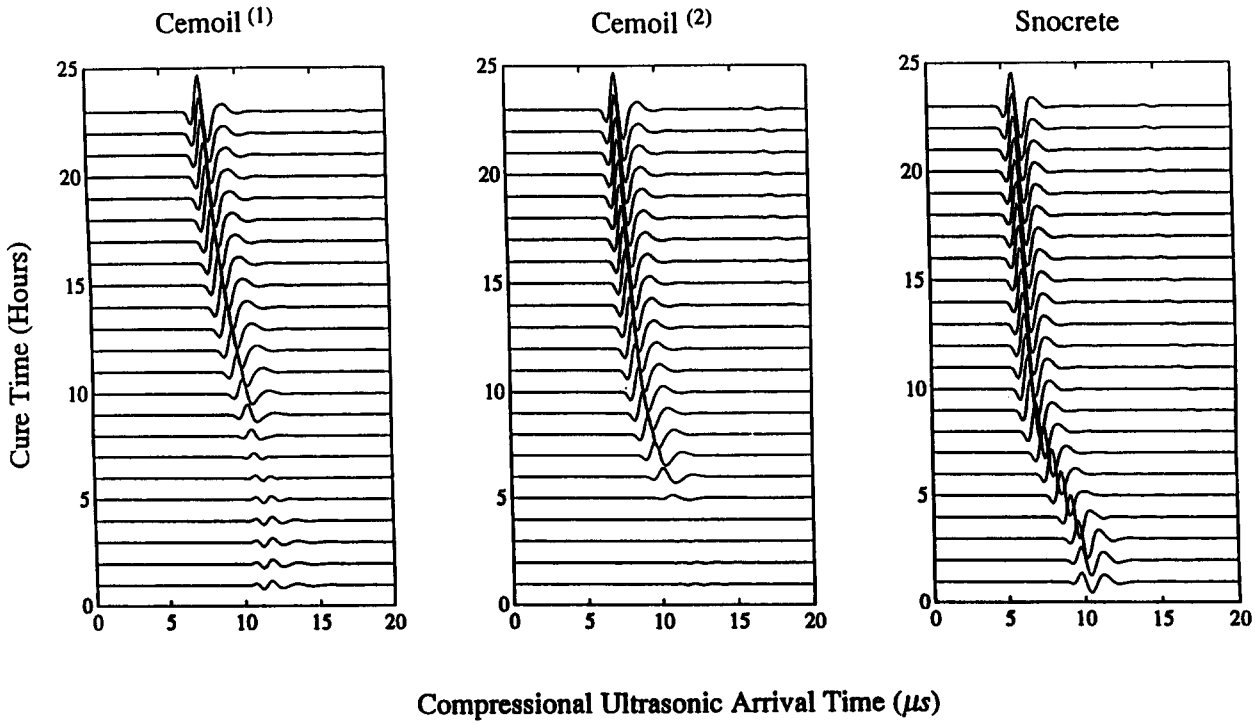

FIGURE 4. The raw compressional wave arrivals are shown for the three cement samples. The axes are labeled as in Figure 3. Here, 20 milliseconds are shown in each case; the initial positions of the windows (i.e., the times at which we begin to display the data) are 18 (Cemoil$^{(1)}$), 18 (Cemoil$^{(2)}$), and 28 milliseconds (Snocrete).

TABLE 1. Comparison of consistometer data with onset times derived from transmitted shear waves for the three cements

Cement	API Thickening Time	Ratio	Shear Wave Onset Time (Filtered)	Ratio	Shear Wave Spectra (300 kHz)	Ratio	Shear Wave Spectra (450 kHz)	Ratio
Cemoil[1]	8.0	1.00	5.60	1.00	6.00	1.00	7.10	1.00
Cemoil[2] (1.4% $CaCl_2$)	5.0	0.63	3.40	0.61	3.90	0.65	4.60	0.65
Snocrete	3.5	0.44	1.90	0.34	2.90	0.48	3.70	0.52

All times are measured in hours. In each of the four cases, the numbers in the Ratio column are obtained by dividing the measured time by the corresponding Cemoil[1] time.

chosen roughly at the center of the late time power spectra. Here, the appearance of shear propagation is seen quite dramatically and the onset times taken from these displays are generally in accord with those obtained from the analysis of first arrival times [Table 1]. We emphasize that the differences between the 300 and 450 kHz data shown in Figure 7 are consistent with the power spectra displayed in Figure 6. Thus, as we shift toward lower frequencies, the transition becomes sharper and moves to slightly earlier cure times. By contrast, the interpretation of the compressional wave power spectra (Figure 8) is less straightforward. The Cemoil[1] and Snocrete samples both show transitions from lower amplitudes at the beginning of the cure to stronger signals at its later stages. Interestingly, these cements show a dip in amplitude just as the shear wave emerges. This interval of attenuation is quite pronounced in the Cemoil[1] case. This observation illustrates the value of simultaneous acquisition of the P and S signals. Note that the amplitude curve for the Cemoil[2] cement is rather different in its behavior, reflecting the very weak compressional signal noted in connection with Figure 4.

Discussion

It is clear that the various estimates of the shear wave onset time given in Table 1 are not equal to the API thickening times of the three cements studied here. We note, however, that the ratios of these quantities (i.e., the ratio of each measured time to the corresponding Cemoil[1] time) are generally in good agreement, the closest accord being obtained when the shear onset time is taken from the 300 kHz transmitted energy data. Since the physical processes involved in the consistometer (thickening time) measurement are so different from those entering the present ultrasonic experiments, the degree of correlation found in Table 1 is quite gratifying. Of course, a much larger number of samples must be studied before any firm conclusions can be drawn regarding the utility of any relation between the thickening time and the shear onset time.

How does this work relate to previous ultrasonic studies of cement hydration? There are a number of articles that document the increase in the compressional wave speed that accompanies the setting of cement paste. Generally their findings are consistent with the results we discussed in connection with Figures 4 and 5. In this connection, the behavior of the

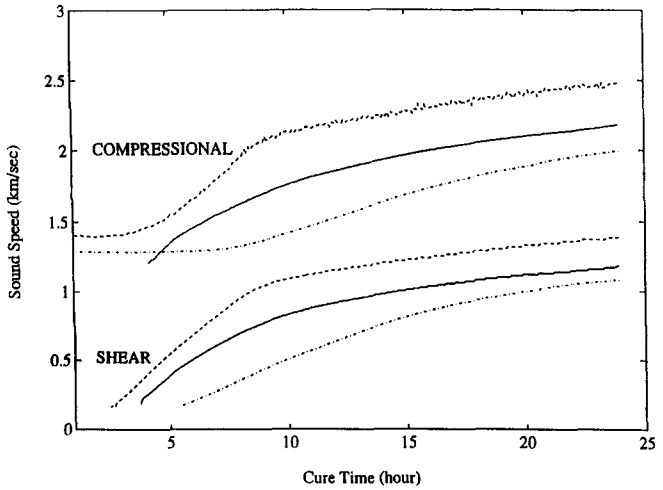

FIGURE 5. The shear and compressional wave speeds (derived from filtered waveforms) are shown as a function of cure time for the three cements: Cemoil[1] (dot-dash), Cemoil[2] (solid), and Snocrete (dash).

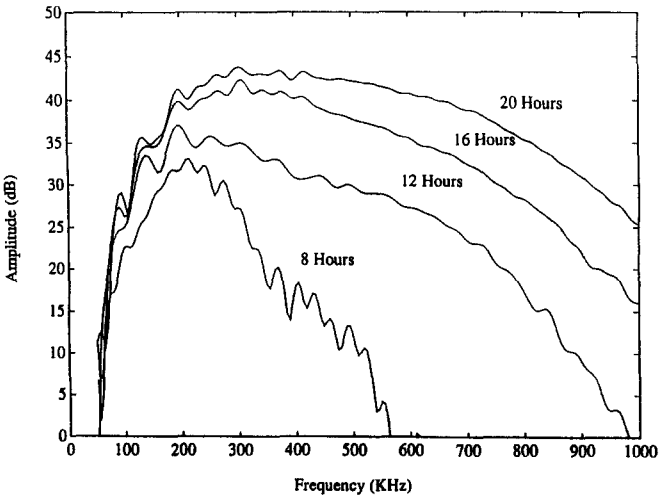

FIGURE 6. The shear wave power spectra are shown at several cure times for Cemoil[1] cement.

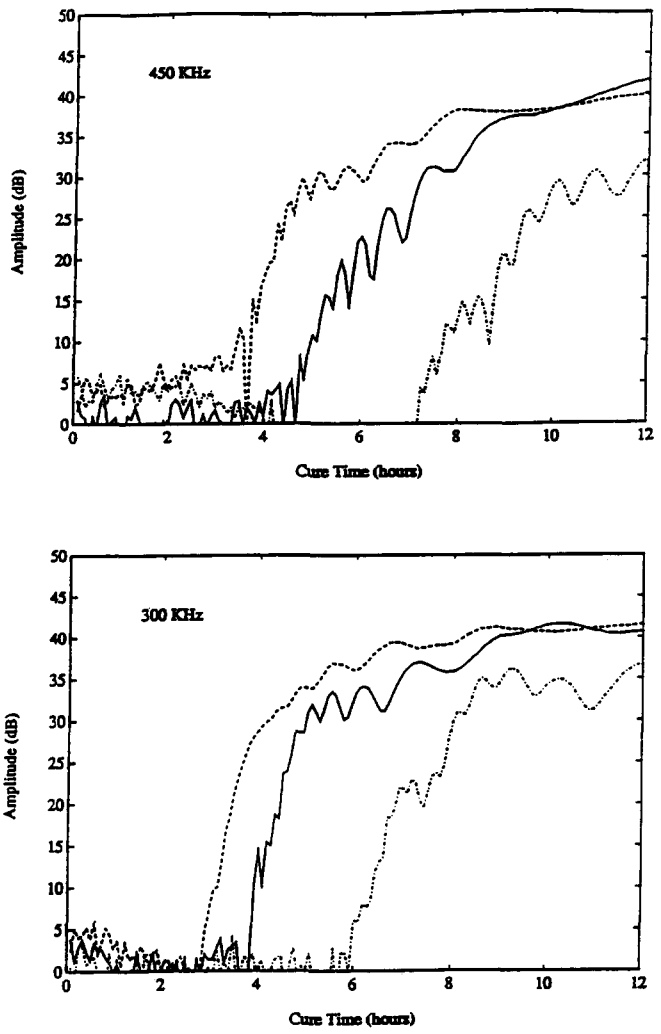

FIGURE 7. The shear wave energy at 450 kHz (top) and 300 kHz (bottom) is shown as a function of cure time for the three cements: Cemoil[1] (dot-dash), Cemoil[2] (solid), and Snocrete (dash).

Cemoil[2] compressional wave appears to be rather anomalous. The only previous work on shear wave propagation in hydrating cements that we are aware of is the article by Stepišnik et al. [9]. Their work is based on an inversion scheme in which the measured complex reflection coefficient (at normal incidence) yields the shear modulus and viscosity. In practice, the phase angles are neglected and only the shear modulus is computed. We believe that the present direct measurements of the shear speed are preferable because the uncertainties associated with their inversion procedure are amplified in the vicinity of the percolation transition. As the transition is approached from below (early cure times), the shear viscosity is expected to diverge; when it is approached from above, the shear modulus vanishes. Both effects lead to large impedance contrasts and to enhanced sensitivity of the calculated results to experimental uncertainties. In addition, the reflection measurements described in ref 9 do not yield any information about shear energy transmission which, as we noted above, provides a particularly clear picture of the transition region.

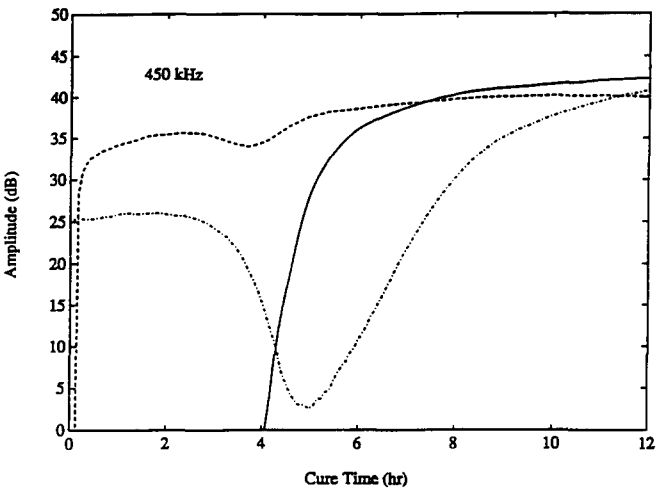

FIGURE 8. The compressional wave energy, at frequency 450 kHz, is shown as a function of cure time for the three cements: Cemoil[1] (dot-dash), Cemoil[2] (solid), and Snocrete (dash). These curves were generated by the same procedure used in Figure 7.

It is also of interest to compare our results with the direct shear modulus data described in refs 10–12. There, low amplitude and essentially zero frequency measurements indicate that cement slurries may show nonvanishing shear moduli at times much earlier than the times measured here for the onset of ultrasonic shear propagation. In particular, such behavior was found for a thixotropic mixture. Indeed, the high sensitivity of their measurements is well suited to probing the earliest stages of the formation of solid-like structures within the slurry. On the other hand, the results in ref 12 for an accelerated class G cement are generally similar to our data on Cemoil[2]. Our approach is, for the most part, complementary to that of ref 12; we are interested in probing the slurry with shear and compressional signals at the same frequency and in studying the correlation between such measurements and consistometer results on the same systems.

Conclusions

The following conclusions can be drawn from this experimental study:

- Our measurement system is capable of detecting the onset of shear arrivals in oil field cements at early stages of their cure process. This onset is considerably more dramatic than the accompanying changes in the compressional wave arrivals.

- An analysis of the frequency components of the acoustic energy provides an especially clear-cut representation of the shear wave onset.
- The shear wave onset appears to be correlated with the API thickening time, the conventional measure of setting time for oil field cements. In some respects this correlation is surprising. Indeed, consistometer measurements have been criticized because the stirring blade is believed to break up the developing frame structure [1,17]. While this mechanism almost certainly contributes to the thickening times being longer than the shear onset times measured here, there nevertheless appears to be a relation between the two quantities. Clearly, many additional measurements are required to assess the validity and importance of this correlation.

Acknowledgment

We have benefited from conversations with E. Garboczi, A. Hayman, T. Hughes, T. Jones, and F. Stanke at various stages of this work.

References

1. Nelson, E.B., Ed. *Well Cementing;* Elsevier Science Publishers: Amsterdam, 1990.
2. API Specification 10, 5th ed.; American Petroleum Institute: Washington, 1990.
3. Munir, Z.A.; Taylor, M.A. *Journal of Materials Science* **1979,** *14,* 640–646.
4. Munir, Z.A.; Taylor, M.A. *Journal of Materials Science* **1979,** *14,* 647–652.
5. Rao, P.P.; Sutton, D.L.; Childs, J.D.; Cunningham, W.C. *Journal of Petroleum Technology* **1982,** 2611–2616.
6. Wilding, C.R. *Journal of Materials Science Letters* **1984,** *3,* 13–14.
7. Kim, H.C.; Yoon, S.S. *Journal of Materials Science* **1988,** *23,* 611–616.
8. Keating, J.; Hannant, D.J.; Hibbert, A.P. *Cement and Concrete Research* **1989,** *19,* 715–26.
9. Stepišnik, J.; Lukač, M.; Kocuvan, I. *Ceramic Bulletin* **1980,** *60,* 481–483.
10. Hannant, D.J.; Keating, J. *Cement and Concrete Research* **1985,** *15,* 605–612.
11. Hannant, D.J.; Dunn, T. *Magazine of Concrete Research* **1980,** *40,* 28–34.
12. Keating, J.; Hannant, D.J.; Hibbert, A.P. *Cement and Concrete Research* **1989,** *19,* 554–566.
13. Sayers, C.M.; Grenfell, R.L. *Ultrasonics* **1993,** *31,* 147–153.
14. Jennings, H.M.; Johnson, S.K. *J. Am. Ceramics Soc.* **1986,** *69,* 790–795.
15. Bentz, D.P.; Garboczi, E.J. In *Material Research Society Symposium Proceedings 195;* Cody, G.D.; Geballe, T.H.; Sheng, P., Eds.; Materials Research Society: Pittsburgh, 1990; pp 523–30.
16. Bentz, D.P.; Coveney, P.; Garboczi, E.J.; Kleyn, M.F.; Stutzman, P.E. *Modelling and Simulation in Materials Science and Engineering* **1994,** in press.
17. Van Kleef, R.P.A.; van Vliet, J.P.M. Paper SPE 20926, presented at Europec 90, The Hague, The Netherlands, October 22–24, 1990.